Modulation of 5-HT_3 receptor desensitization by the light chain of microtubule-associated protein 1B expressed in HEK 293 cells

Hui Sun[1], Xiang-Qun Hu[1], Michel B. Emerit[2], Jeffrey C. Schoenebeck[1], Cassin E. Kimmel[1], Robert W. Peoples[3], Angela Miko[1] and Li Zhang[1]

[1]*Laboratory for Integrative Neuroscience, National Institute on Alcohol Abuse and Alcoholism, National Institutes of Health, 5625 Fishers Lane, Bethesda, MD 20892, USA*
[2]*INSERM U677, Neuropsychopharmacologie Moléculaire, Cellulaire et Fonctionelle, C.H.U. Pitié-Salpêtrière, 91 Bd de l'Hôpital, 75634 Paris Cedex 13, France*
[3]*Department of Biomedical Sciences, College of Health Sciences, Marquette University, Milwaukee, WI 53201-1881, USA*

Regulation of ligand-gated ion channel (LGIC) function and trafficking by cytoskeleton proteins has been the topic of recent research. Here, we report that the light chain (LC1) of microtubule-associated protein 1B (MAP1B) specifically interacted with the 5-HT_{3A} receptor, a predominant serotonin-gated ion channel in the brain. LC1 and 5-HT_{3A} receptors were colocalized in central neurons and in HEK 293 cells expressing 5-HT_{3A} receptors. LC1 reduced the steady-state density of 5-HT_{3A} receptors at the membrane surface of HEK 293 cells and significantly accelerated receptor desensitization time constants from 3.8 ± 0.3 s to 0.8 ± 0.1 s. However, LC1 did not significantly alter agonist binding affinity and single-channel conductance of 5-HT_{3A} receptors. On the other hand, application of specific LC1 antisense oligonucleotides and nocodazole, a microtubule disruptor, significantly prolonged the desensitization time of the recombinant and native neuronal 5-HT_3 receptors by 3- to 6-fold. This kinetic change induced by nocodazole was completely rescued by addition of LC1 but not $GABA_A$ receptor-associated protein (GABARAP), suggesting that LC1 can specifically interact with 5-HT_{3A} receptors. These observations suggest that the LC1–5-HT_{3A} receptor interaction contributes to a mechanism that regulates receptor desensitization kinetics. Such dynamic regulation may play a role in reshaping the efficacy of 5-HT_3 receptor-mediated synaptic transmission.

(Received 6 July 2007; accepted after revision 21 November 2007; first published online 6 December 2007)
Corresponding author L. Zhang: Laboratory for Integrative Neuroscience, National Institute on Alcohol Abuse and Alcoholism, National Institutes of Health, 5625 Fishers Lane, TS24, Bethesda, MD 20892, USA.
Email: lzhang@mail.nih.gov

Most ligand-gated ion channel (LGIC) proteins are anchored to the cytoskeleton network by bridging proteins at synaptic sites (Betz, 1990; Ortells & Lunt, 1995). This linkage appears to be critical for receptor targeting, clustering and trafficking (Hanley *et al.* 1999; Wang *et al.* 1999; Sheng & Pak, 2000; Moss & Smart, 2001). In addition to regulating receptor trafficking, the receptor–cytoskeleton linkage has been shown to be important for channel gating properties such as desensitization kinetics and single-channel conductance (Billups *et al.* 2000; Chen *et al.* 2000; Everitt *et al.* 2004; Boileau *et al.* 2005; Luu *et al.* 2006). In the continued presence of agonists, most LGICs desensitize. The desensitization plays a critical role in the regulation of the shape and efficacy of synaptic transmission (Jones & Westbrook, 1995, 1996; Overstreet *et al.* 2000). While most previous studies of receptor desensitization focused on ligand binding and channel pore domains (Corringer *et al.* 1998; Gunthorpe *et al.* 2000; Bohler *et al.* 2001; Sun *et al.* 2002), recent research interest has turned to the role of cytoskeleton proteins in the regulation of the receptor desensitization process. For instance, γ-aminobutyric acid type A ($GABA_A$) receptor-associated protein (GABARAP) regulates $GABA_A$ receptor gating kinetics by altering steady-state receptor density at the cell membrane surface and agonist binding affinity (Chen *et al.* 2000; Petrini *et al.* 2003; Boileau *et al.* 2005). Similar observations have been reported in studies of the microtubule interaction with *N*-methyl-D-aspartate (NMDA), glycine and nicotinic acetylcholine (nACh) receptors (Lopez & McKay, 1997; van Rossum *et al.* 1999; Van Zundert *et al.* 2004; Washbourne *et al.* 2004; Yuen *et al.* 2005).

 DOI: 10.1113/jphysiol.2007.136440

The serotonin type 3 (5-HT_3) receptor is a member of a cys-loop LGIC superfamily, which includes nicotinic acetylcholine (nACh), $GABA_A$ and glycine receptors (Maricq *et al.* 1991). Activation of 5-HT_3 receptors is found to modulate the release of neurotransmitters such as dopamine in the meso-cortico-limbic system (van Hooft & Vijverberg, 2000). Of all five 5-HT_3 subunits identified by molecular cloning, the 5-HT_{3A} subunit has been the most thoroughly characterized (Zhang & Lummis, 2006). The 5-HT_{3A} subunit can form a functional channel, which is thought to be the major functional form in the central nervous system (CNS) (Zhang & Lummis, 2006). Like other members of the LGIC superfamily, 5-HT_3 receptors desensitize in the prolonged presence of 5-HT (Yakel & Jackson, 1988; Hu *et al.* 2006). Despite extensive investigation, the molecular mechanisms of receptor desensitization are not totally understood. Both the large extracellular N-terminal domain and transmembrane domains of LGICs have been found to be important in the regulation of 5-HT_{3A} receptor desensitization (Hu *et al.* 2003). A recent study from our laboratory has shown that the large cytoplasmic domain of the 5-HT_{3A} receptor is also involved in the regulation of 5-HT_{3A} receptor desensitization kinetics (Hu *et al.* 2006).

Less is known about the interaction between cytoskeleton proteins and 5-HT_{3A} subunits. The 5-HT_{3A} subunits and F-actin cytoskeleton are colocalized and coclusterized in various neurons and cell lines (Emerit *et al.* 2002). F-actin is also involved in the modulation of the 5-HT_{3A} receptor function and trafficking by activation of protein kinase C (Sun *et al.* 2003). However, whether or not cytoskeleton proteins can regulate 5-HT_3 receptor gating kinetics has not been reported. Using yeast two-hybrid to screen a mouse brain cDNA library, we have identified a specific interaction between the light chain (LC1) of microtubule-associated protein 1B (MAP1B) and the 5-HT_{3A} receptor. LC1 was colocalized with 5-HT_{3A} subunits in central neurons, especially in growth cone axons. We have also provided evidence showing that LC1 accelerated 5-HT_{3A} receptor desensitization and reduced steady-state receptor density at the cell membrane surface when expressed in HEK 293 cells.

Methods

Yeast two-hybrid screen

Bait plasmids were constructed by amplifying cDNA fragments encoding the large intracellular domains of 5-HT_{3A}, 5-HT_{3B}, nAChα7, α4, $GABA_A\alpha$1, β1, γ2 and $GABA_C\rho$1 subunits using polymerase chain reaction (PCR). The amplified fragments were subcloned into a Gal4-DNA-binding domain vector, pACT2 (Clontech, Mountain View, CA, USA), at appropriate enzyme restriction sites. A similar procedure was used to construct deletional mutations in the Large intracellular loop (LIL) of 5-HT_{3A} receptors. The authenticity of the DNA sequence of all constructs was confirmed by double-strand DNA sequencing using an ABI Prism 377 automatic DNA sequencer (Applied Biosystems, CA, USA). A mouse fetal brain cDNA library constructed in the Gal4 activation domain was screened with the bait plasmids. The plasmids were transformed into yeast strain Y190 and transformants were selected on triple-dropout media (–Leu/–Trp/–His) and further examined for β-galactosidase activity.

Cell culture and transfection

The methods for handling the animals and preparation of primary neuronal cultures conformed to institutional guidelines, and were approved by the Animal Care and Use Committee of the NIAAA Division of Intramural Clinical and Basic Research.

Hippocampal neuron cultures were prepared using fetuses from female Sprague–Dawley rats on day 18 of gestation. Rats and E18 fetuses were killed by inhalation of a rising concentration of CO_2 and hippocampi of rat fetuses were dissected. Neuronal cultures were prepared using a modified previously described procedure (Emerit *et al.* 2002). Dissociation was achieved with a Pasteur pipette after trypsinization. Cells were counted and plated on poly L-lysine (50 μg ml^{-1})-coated 15 mm diameter coverslips (Electron Microscopy Sciences, Hatfield, PA, USA), at a density of 20 000–40 000 cells per 15 mm dish (100–200 cells mm^{-2}), in complete Neurobasal medium supplemented with B27 (Invitrogen, Carlsbad, CA, USA) containing 1 mM L-glutamine, 25 μM β-mercaptoethanol and penicillin G (10 U ml^{-1})–streptomycin (10 mg ml^{-1}). Four hours after plating, the coverslips were transferred to a 90 mm dish containing conditioned medium obtained by incubating the complete Neurobasal medium described above on a glial culture (70–80% confluency) for 24 h. The medium was partially changed every 3–4 days. The plasmid cDNA of YFP-5-HT_{3A}R was transfected in a ratio 3 : 1 using Lipofectamine 2000 (Invitrogen). The transfection efficiency of the cDNA was 15–20%. Human embryonic kidney (HEK 293) cells cultured as previously described (Hu *et al.* 2003) were cotransfected with the cDNAs of 5-HT_{3A}-His6-Flag and LC1-GFP using Lipofectamine 2000. N1E115 cells (American Type Culture Collection) were prepared according to a previously described method (Van Hooft & Vijverberg, 1995).

Immunocytochemistry

Immunofluorescence was performed 2–7 days after transfection for neurons. The cDNA of YFP-5-HT_{3A} receptor was generated as previously described (Grailhe *et al.* 2004). Extracellular labelling of the YFP and

Flag epitope was performed with using monoclonal anti-GFP–anti-rabbit-AF488 Red (Sigma-Aldrich: 1 : 1000) and anti-Flag M2 antibody (Sigma, 1 : 5000), for 2 h at room temperature, and revealed with AlexaFluor 568-conjugated donkey anti-mouse IgG (Molecular Probes), at 1 : 1000 dilution, for 1 h at room temperature. Immunofluorescence images were generated using a Leica TCS-400 laser scanning confocal microscope. Contrast and brightness were chosen to ensure that all relevant pixels were within linear range. Images are the product of a 16-fold line average. For double-labelling experiments, pictures were generated using Adobe Photoshop 7.0. Representative cells were chosen for the pictures.

Western blot

The membrane surface proteins of 5-HT$_{3A}$ receptors expressed in HEK 293 cells were isolated by a biotin-labelling method as previously described (Sun *et al.* 2003). Labelled proteins were eluted from the beads and loaded onto 10% SDS/PAGE and transferred to a polyvinylidine difluoride membrane (Invitrogen). The membranes were incubated for 1 h with a polyclonal antibody (pAb120, 1 : 4000) directed to the extracellular N-terminal domain of the 5-HT$_{3A}$ receptor (Spier *et al.* 1999).

Receptor binding

The cells were incubated at 37°C for 2 h in various concentrations of [^{3}H]LY 278,584 solution (specific activity = 64 Ci mmol^{-1}; Amersham Biosciences), and then washed thoroughly with PBS solution to remove free [^{3}H] ligands. The non-specific binding was determined by incubation in 300 μM unlabelled 5-HT. The specific binding was determined by subtracting the non-specific binding from the total binding. Each data point is the average from at least 3–4 separate experiments. The radioactivity (c.p.m.) of each sample was determined in a 1409 DSA Wallac liquid scintillation counter (Perkin-Elmer Life Science). K_d and B_{max} were determined by equilibrium and competitive binding data using Prism Software (GraphPad Software, San Diego, CA, USA).

Antisense oligo synthesis, delivery and characterization

The sequences of the LC1 antisense oligonucleotide (ATS) and its inverted control are 5′-TCGAGGAGTTCTCACCTGCATGTTG-3′ and 5′-GTTGTACGTCCACTCTTGAGGAGCT-3′. They were synthesized and modified as morpholino oligos with 3′ ends labelled with biotin (Gene Tools, LLC, Philomath, OR, USA). The morpholino oligos were delivered into HEK 293 cells using a special delivery system that contains ethoxylated polyethylenimine, a weakly basic delivery reagent (Gene Tools, LLC). A reverse-transcription (RT) PCR was conducted to verify the mRNA of LC1 in HEK 293 cells with or without the LC1-ATS treatment for 16 h. The sequences of the primers used RT-PCR were 5′-AAAGTGTCCAGGGTGGCTTC-3′ (human MAP1B, 6850–6870) and 5′-CTCCTGGTACCATTCCCTCA-3′ (human MAP1B, 7304–7284). The quantitative level of MAP1B mRNA was determined by two steps TaqMan real-time PCR assay. Human β-actin was used as an endogenous control for normalization. The PCR reaction was performed at 50°C for 2 min, 95°C for 10 min, 95°C for 15 s and 60°C for 1 min for 40 cycles using an ABI 7700 Sequence Detector (Applied Biosystems, Foster City, CA, USA). Fluorescence signal data were collected after each PCR cycle and analysed using Sequence Detector System software, version 1.6 (Applied Biosystems).

Kinetic analysis

Transient transfection of HEK 293 cells was carried out using Lipofectamine 2000 reagent (Invitrogen). The cDNA plasmid ratio for 5-HT$_{3A}$ and LC1 was 1 : 1 (total amount of DNA: 1.5 μg). The currents were recorded 1–3 days after transfection. Cells were continuously superfused with a solution containing 140 mM NaCl, 5 mM KCl, 1.8 mM $CaCl_2$, 1.2 mM $MgCl_2$, 5 mM glucose, and 10 mM Hepes (pH 7.4 with NaOH; ~340 mosmol l^{-1} with sucrose). Membrane currents were recorded in the whole-cell configuration using an Axopatch 200B amplifier (Axon) at 20–22°C (Hu *et al.* 2006). Cells were held at −60 mV unless otherwise indicated. Data were acquired using pCLAMP 8 software (Molecular Devices, Sunnyvale, CA, USA). Bath solutions were applied through two-barrel theta glass tubing (TGC150, Warner Instruments, Hamden, CT, USA) that had been pulled to a tip diameter of ~200 μm. A piezoelectric device was driven by transistor–transistor logic pulses from the pCLAMP 8 software. Voltage applied to the piezoelectric device produced a rapid lateral displacement of the theta tubing to move the interface between control and test solutions. The solution exchange rate was estimated using the potential change induced by switching from the control solution to a 140 mM *N*-methyl-D-glucamine test solution. The solution exchange time constants were ~0.3 ms for an open pipette tip and 1.6 ms for whole-cell recording.

Noise analysis

Single-channel conductance was determined using noise analysis (Hu *et al.* 2006). Data were acquired at 5–10 kHz in 1 s blocks on a computer using a DigiData interface and pCLAMP software (Molecular Devices). Records of current activated by 1 μM 5-HT were filtered (2 kHz 8-pole Butterworth) and the DC component digitally

subtracted. Variance of the AC component was determined and the background variance subtracted as previously described (Brown *et al.* 1998) and plotted against background-corrected mean current amplitude from the DC component, and the unitary current was determined from a linear fit to the data. Values for unitary current (in pA) were divided by the holding potential minus the reversal potential (in mV) to yield single-channel conductance (in pS).

Data analysis

Concentration–response curves were fitted by the Hill equation:

$$I/I_{max} = 1/[1 + (EC_{50}/[Agonist])^n] \quad (1)$$

where I is the current amplitude activated by a given concentration of agonist [agonist]; I_{max} is the maximal response of the cell, n is the Hill slope, and EC_{50} is the concentration eliciting a half-maximal response. Statistical analysis of concentration–response data was performed using the non-linear curve-fitting program Prism. Kinetic analysis was performed using Origin 6.0 (Microcal), pCLAMP 8.0 (Molecular Devices) or Statistica 5.5 (Statistica, StatSoft) software. The time constants of activation, deactivation and desensitization were determined with Levenberg–Marquardt algorithms. The desensitization and deactivation kinetics of 5-HT_{3A} receptors were best-fitted to a mono-exponential function when expressed in HEK 293 cells. However, a bi-exponential function was required to adequately fit the desensitization decays of current activated by 5-HT in N1E115 cells and in HEK 293 cells after cotransfection of 5-HT_{3A} receptors with LC1. In this scenario, a weighted summation of the fast and slow components was used with the following formula:

$$(A_{FAST} \times \tau_{FAST} + A_{SLOW} \times \tau_{SLOW}) \quad (2)$$

where τ_{FAST} and τ_{SLOW} were the fast and slow decay time constants, and A_{FAST} and A_{SLOW} were the relative proportions of the fast and slow component.

Results

A specific interaction between the light chain (LC1) of MAP1B and 5-HT_{3A} receptor

To investigate if 5-HT_{3A} receptors can interact with cytoskeleton proteins, we screened a mouse fetal brain cDNA library using the yeast two-hybrid method with a bait encoding the large intracellular domain of the 5-HT_{3A} receptors. We identified several clones that strongly interacted with the bait protein. The interacting clones were identical and encoded nearly the entire open reading frame of the light chain (LC1) of microtubule-associated protein 1B (MAP1B) (Fig. 1*A*). To localize the molecular domains of the receptor proteins that interact with LC1, we divided the large intracellular domain of the 5-HT_{3A} receptor into two segments, the 5′ end (325–395) and 3′ end (395–464) segments (Fig. 1*B*). These clones were used to produce fusion proteins with Gal4 in yeast. Deletion of the 3′ end (395–464) domain resulted in a loss of the interaction between LC1 and the 5-HT_{3A} subunit in yeast, suggesting that the 3′ end domain is critical for the interaction with LC1. To determine if the interaction with LC1 is selective for the 5-HT_{3A} subunit over other members of this superfamily of LGICs, we constructed bait proteins from the intracellular domains of the 5-HT_{3B} subunit, nAChα7 and α4 subunits, $GABA_A$ α1, β1 and γ2 subunits, $GABA_C$ ρ1 and glycine α1 subunits (Fig. 1*C*). All of these constructs yielded fusion proteins with the expected molecular masses verified by Western blot analysis (data not shown). Besides the 5-HT_{3A} subunit, the glycine receptor α1 subunit was also found to interact with LC1. However, no interaction was found between the ρ1 subunit of $GABA_C$ receptor and LC1 even though

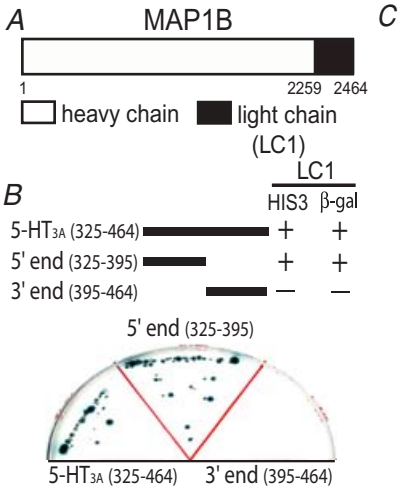

C

Bait proteins		Growth on -His/-Trp/-Leu
5-HT_{3A}	(302-441)	+
5-HT_{3B}	(315-415)	—
nAChα7	(318-469)	—
nAChα4	(331-600)	—
$GABA_{A\alpha1}$	(335-420)	—
$GABA_{A\beta1}$	(330-451)	—
$GABA_{A\gamma2}$	(356-442)	—
$GABA_{C\rho1}$	(364-452)	—
$Gly_{\alpha1}$	(309-392)	+

Figure 1. Identification of an interaction between LC1 and 5-HT_{3A} receptor
A, schematic illustration of a cloned MAP1B-LC1. *B*, schematic illustration of the entire (325–464) and segmental LILs of the 5-HT_{3A} subunit. These constructs were cotransformed with LC1 into yeast strain Y190 in a triple dropout media (–Leu/–Trp/–His). Interactions between the LC1 and the LIL of the 5-HT_{3A} receptor and its truncated fragments in yeast, as measured by growth on –His/–Leu/–Trp medium and β-galactosidase activity. *C*, interaction of MAP1B-LC1 with the LILs of various LGICs in yeast, as measured by growth on –His/–Leu/–Trp medium.

the ρ1 subunit has been reported to strongly interact with the heavy chain of MAP1B (Hanley *et al.* 1999). Moreover, we did not observe any interaction between LC1 and other members of the LGIC proteins listed in Fig. 1C.

Colocalization of LC1 with 5-HT$_{3A}$ receptors

As a neuron-specific protein, LC1 is highly expressed at the early neuronal developmental stage (Hammarback *et al.* 1991). To reveal if LC1 is colocalized with 5-HT$_{3A}$ receptors in native central neurons, we transfected the cDNA of YFP-5-HT$_{3A}$ receptor into hippocampal neurons isolated from 18 day rat embryos. The YFP is connected to the extracellular N-terminus of 5-HT$_{3A}$ receptor (Grailhe *et al.* 2004), which allows us to intensify the fluorescence signal by adding extracellular labelling cell surface expression of the 5-HT$_{3A}$ receptors with anti-GFP antibody. In agreement with previous studies (Kawakami *et al.* 2003; Bouquet *et al.* 2004; Del Rio *et al.* 2004), MAP1B was highly expressed in distal neurites such as adhesion and branching spots along growing axons (Fig. 2*A* and *B*). In these areas, 5-HT$_{3A}$ receptor clusters appeared to be consistently colocalized with LC1. Moreover, coaccumulation of YFP-5-HT$_{3A}$ receptor clusters and LC1 was always observed in the central part of growth cones. Consistent with a previous study (Emerit *et al.* 2002), 5-HT$_{3A}$ receptors were mainly distributed in the microstructures of cell plasma membranes when expressed in HEK 293 cells (Fig. 2*C* and *D*). The colocalization of 5-HT$_{3A}$ receptor-His6-Flag with LC1-GFP was apparent in microstructures of the cells such as lamellipodia and filapodia (Fig. 2*C* and *D*).

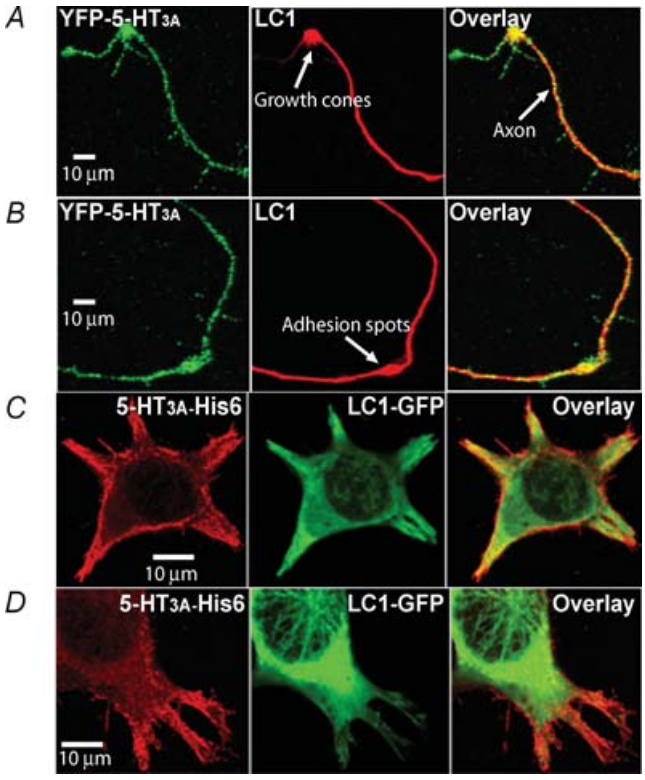

Figure 2. Colocalization of 5-HT$_{3A}$ receptors with LC1
A and *B*, different examples of imaging illustrating colocalization of 5-HT$_{3A}$ receptors and LC1 in neurons. Hippocampal neurons were cultured in a serum-free medium for 4 days and transfected with the cDNA of the YFP-5-HT$_{3A}$ receptor. *C* and *D*, colocalization of 5-HT$_{3A}$ receptors and LC1 in HEK 293 cells. 5-HT$_{3A}$-His6-Flag and LC1-GFP were cotransfected into HEK 293 cells. The red is the labelling of 5-HT$_{3A}$ receptor protein with anti-Flag-M2-Ab/anti-AlexaFluor 568. The green is the fluorescence from LC1-GFP.

LC1 reduces surface expression of 5-HT$_{3A}$ receptors

Previous studies have shown that GABARAP can regulate GABA$_A$ receptor channel density at the cell surface (Leil *et al.* 2004; Boileau *et al.* 2005). In view of this, we investigated whether or not LC1 can modulate 5-HT$_{3A}$ receptor density at the cell membrane surface. We first measured the surface expression level of 5-HT$_{3A}$ receptor proteins by labelling the cell surface with sulfo-NHS-SS-biotin. The representative Western blot shows that expression of LC1 reduced the apparent density of 5-HT$_{3A}$ receptor proteins expressed at the surface but not total membranes of HEK 293 cells (Fig. 3*A*).

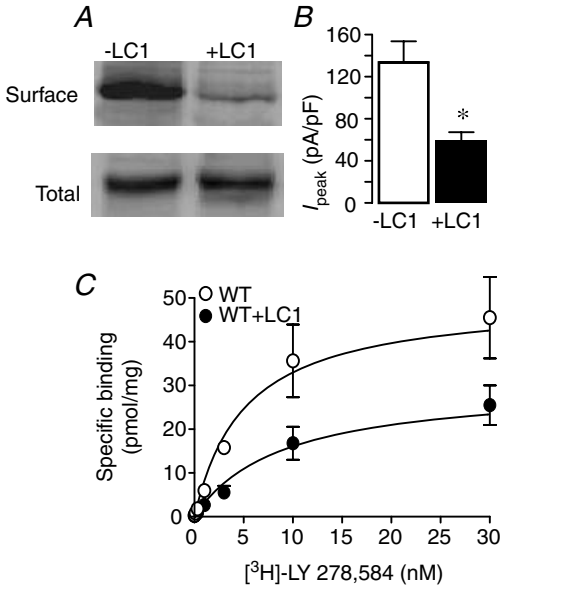

Figure 3. Internalization of 5-HT$_{3A}$ receptors by LC1
A, Western blot of surface and total membrane fractions of 5-HT$_{3A}$ receptors expressed in HEK 293 cells without and with LC1 cotransfection. *B*, bar graph represents the mean current density without (open bar) and with (filled bar) LC1. Each data point represents mean ± S.E.M. from 11 cells. Asterisk indicates a significant difference from control (unpaired *t* test, $P = 0.001$). *C*, specific [^{3}H]LY 278,584 binding for 5-HT$_{3A}$ receptors expressed in HEK 293 cells without (○) and with (●) coexpression of LC1. The specific binding is determined by subtracting non-specific binding (determined with 300 μM non-radiolabelled 5-HT) from total binding. Error bars that are not visible are smaller than the symbols.

Consistent with this, we observed that LC1 reduced the range of peak current activated by 30 μM 5-HT from 340–2280 pA ($n = 11$) to 230–1000 pA ($n = 11$). The mean current density (MCD) was estimated by plotting peak current over capacitance. The average values of MCD were 133 ± 20 pA pF^{-1} and 58 ± 9 pA pF^{-1} in the absence and presence of LC1. These values were significantly different (Fig. 3*B*, $P = 0.001$). This difference appeared to be specific for LC1 since coexpression of GABARAP with 5-HT$_{3A}$ subunits did not significantly affect the amplitude of current activated by maximal 5-HT (data not shown). Next, we conducted receptor-binding experiments to examine the effect of LC1 on the B_{max} of receptor binding. As illustrated in Fig. 3*C*, LC1 significantly reduced the B_{max} value of specific [^{3}H]LY 278,584, a selective antagonist of 5-HT$_3$ receptor, binding from 59 ± 5 pmol (mg protein)$^{-1}$ to 30 ± 3 pmol (mg protein)$^{-1}$ ($P < 0.001$, $n = 9$). The K_d values were 6 ± 0.6 nM and 5.6 ± 0.3 nM, respectively, for the 5-HT$_{3A}$ receptors without and with LC1. These values are not significantly different (unpaired *t* test, $P = 0.2$). These results indicate that LC1 reduces 5-HT$_{3A}$ receptor density at the cell surface without significantly altering the binding affinity to LY 278,584.

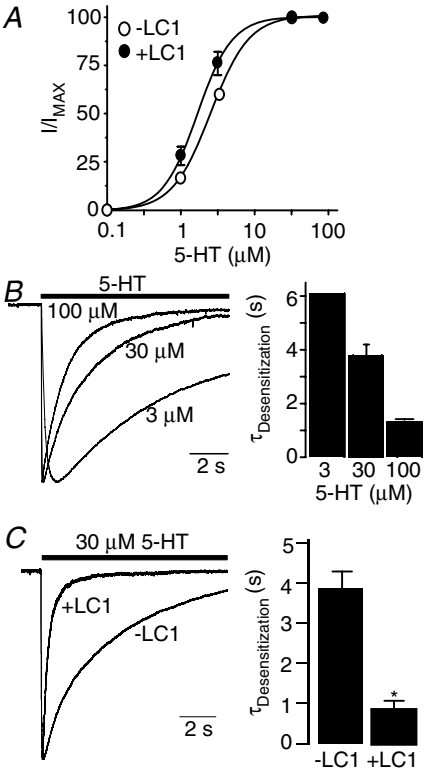

Figure 4. Expression of LC1 accelerates 5-HT$_{3A}$ receptor gating kinetics by LC1

A, 5-HT concentration–response curves for 5-HT$_{3A}$ receptors expressed in cells without and with coexpression of LC1. *I* and I_{MAX} represent the current activated by the given and maximal concentrations of agonist, respectively. Each data point represents the mean ± S.E.M. from 6–9 cells. Error bars that are not visible are smaller than the symbols. *B*, desensitization kinetics of 5-HT$_{3A}$ receptors expressed in HEK 293 cells. The representative tracings represent the desensitization decay of the normalized peak currents in the presence of various concentrations of 5-HT. Bar graph represents average desensitization time constants of 5-HT$_{3A}$ receptors. Each bar represents mean ± S.E.M. from at least 5 cells. *C*, acceleration of 5-HT$_{3A}$ receptor desensitization by LC1. Each bar represents mean ± S.E.M. from 6–7 cells. Asterisk indicates a significant difference from control group (unpaired *t* test, $P < 0.001$).

LC1 accelerates 5-HT$_{3A}$ receptor desensitization kinetics

Expression of LC1 in HEK 293 cells slightly shifted in parallel the 5-HT concentration–response curve to the left (Fig. 4*A*). The 5-HT EC_{50} values are 2.7 ± 0.42 μM and 1.8 ± 0.3 μM without and with coexpression of LC1. These values are not significantly different (unpaired *t* test, $P = 0.1$, $n = 5$). To determine the effect of LC1 on the gating properties of 5-HT$_{3A}$ receptors, we conducted a kinetic analysis using a fast perfusion system in HEK 293 cells expressing 5-HT$_{3A}$ receptors. The gating kinetics of 5-HT$_{3A}$ receptors have been well documented in this system. In line with previous observations (Gunthorpe *et al.* 2000; Hu *et al.* 2003), the average desensitization constants of currents activated by 3, 30 and 100 μM 5-HT were 6.1 ± 0.18 s, 3.8 ± 0.4 s and 1.3 ± 0.02 s (Fig. 4*B*). These constants were best described by a mono-exponential function. The desensitization constant of current activated by 30 μM 5-HT was remarkably faster in cells coexpressing LC1 (Fig. 4*C*) and exhibited two components. The fast component contributed 74% of total current decay for 5-HT. The slow component was still significantly faster than the single component of current decay in the absence of LC1 coexpression ($P < 0.001$). To properly evaluate the desensitization kinetics, we normalized the fast and slow components into a weighted summation using a formula described in Methods.

LC1-ATS slows 5-HT$_{3A}$ receptor desensitization

Antisense oligonucleotides (ATS) have proved to be a valuable tool to uncover the functional identity of endogenous proteins (Kirsch *et al.* 1993). We therefore designed a morpholino antisense oligonucleotide in an attempt to disrupt RNA splicing of LC1 by targeting the exon 10–intron boundary of MAP1B (Fig. 5*A*). The 3′ end of the oligonucleotides was labelled with biotin so that the labelled oligonucleotides could be readily visualized after delivery into HEK 293 cells. To characterize the efficacy of this antisense oligo, we conducted the following experiments. We first examined the structure of the targeted mRNA region by RT-PCR of the cells treated with LC1-ATS. The RT-PCR produced a fragment with a molecular size smaller than that of the inverted control (Invert) (Fig. 5*B*), indicating that LC1-ATS disrupts the normal splicing process of LC1 in HEK 293 cells. We also

performed real-time quantitative PCR to investigate if LC1-ATS treatment can alter the expression level of endogenous MAP1B mRNA in HEK 293 cells. Pretreatment of the cells with LC1-ATS significantly reduced the expression level of MAP1B mRNA by 81% (Fig. 5*C*; unpaired *t* test, $P < 0.001$, $n = 9$). Pretreatment of the cells expressing 5-HT$_{3A}$ receptors with LC1-ATS did not significantly alter the EC_{50} value of the 5-HT concentration–response curve (2.4 ± 0.42 μM *versus* 2.7 ± 0.4 μM, unpaired *t* test, $P = 0.4$, $n = 4$). Application of LC1-ATS did not significantly affect receptor activation kinetics (Fig. 5*D*, unpaired *t* test, $P = 0.2$, $n = 6$). However, LC1-ATS significantly slowed microscopic current decay in the presence of 30 μM 5-HT (Fig. 5*E*). The average desensitization time courses of the 5-HT-activated current were 3.8 ± 0.12 s and 9.94 ± 0.83 s without and with LC1-ATS pretreatment (Fig. 5*E*). These values were significantly different (unpaired *t* test, $P < 0.01$, $n = 7$). In contrast, pretreatment of the cells with the inverted control did not significantly alter the desensitization kinetics of 5-HT$_{3A}$ receptors (Fig. 5*E*), suggesting that modulation of the channel properties by LC1-ATS is specific for LC1.

Nocodazole treatment slows receptor desensitization

The above observations indicate that LC1 is involved in the regulation of 5-HT$_{3A}$ receptor gating kinetics. One of the key biological functions of LC1 is to stabilize microtubules. Accumulating evidence has suggested that certain types of LGICs are linked to microtubule skeletons by associated proteins (Moss & Smart, 2001; Chen & Olsen, 2007). In this regard, we predicted that disruption of microtubules should produce the opposite effect on 5-HT$_{3A}$ receptor gating kinetics if LC1 links the receptors to microtubules. To test this hypothesis, we preincubated HEK 293 cells expressing 5-HT$_{3A}$ receptors with 10 μM nocodazole, a microtubule disruptor, for 4 h and washed the cells thoroughly prior to electrophysiological recording. Nocodazole treatment significantly slowed the time constant of 5-HT$_{3A}$ receptor desensitization by 2.9-fold (Fig. 6*A*, unpaired *t* test, $P < 0.001$). Similar kinetic change was not observed in cells treated with 10 μM cytochalasin D and B, microfilament disruptors (data not shown), suggesting that F-actin may not be involved in the regulation of 5-HT$_{3A}$ receptor gating kinetics. We also observed that nocodazole treatment did not significantly alter the EC_{50} value for 5-HT (2.9 ± 0.3 μM *versus* 2.7 ± 0.42 μM ($P = 0.2$, unpaired *t* test, $n = 5$). In addition, simultaneous application of 25 μM nocodazole did not significantly alter the desensitization time constants (3.7 ± 0.3 s *versus* 3.5 ± 0.2 s) of 5-HT$_{3A}$ receptors expressed in HEK 293 cells. This suggests that the modulation of the receptor desensitization by nocodazole pretreatment is due to a direct drug–receptor interaction. Next, we asked if the nocodazole-induced gating alteration can be replicated in native 5-HT$_3$ receptor–channels in N1E115 cells. In these cells, the desensitization kinetics of 5-HT$_{3A}$ receptors exhibited two time constants, fast and slow components (Fig. 6*B*). The fast decay of the current in the presence of 30 μM 5-HT was 0.25 s and the slow decay was 3.2 s.

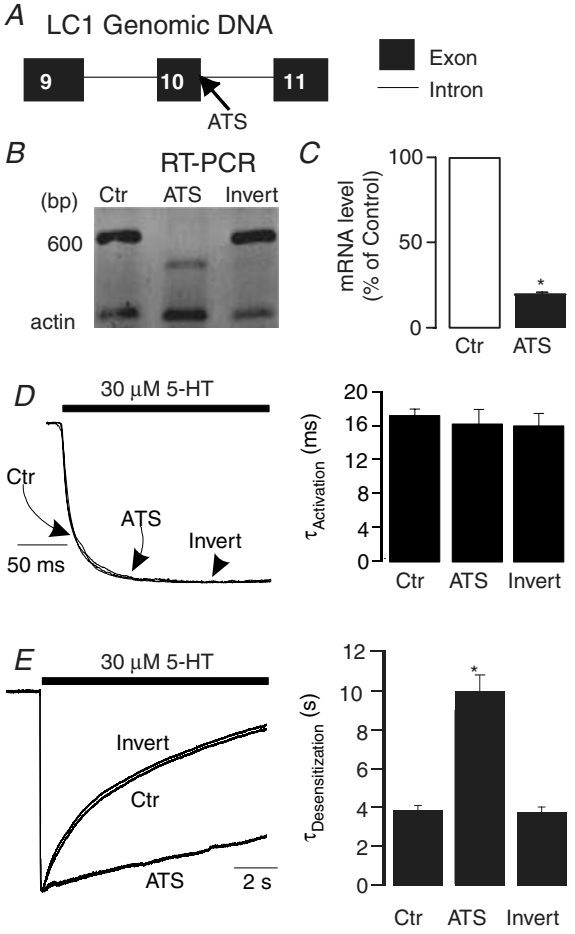

Figure 5. Modulation of 5-HT$_{3A}$ receptor–channel properties by LC1 antisense oligonucleotides
A, schematic illustration of the genomic structure of MAP1B-LC1. Note that the LC1 antisense oligo (ATS) is designed to target a segment crossing an axon (10)–intron border. *B*, RT-PCR of endogenous LC1 in HEK 293 cells after LC1-ATS and inverted control treatment. *C*, quantization of MAP1B mRNA by real-time PCR in HEK 293 cells after LC1-ATS treatment. The relative expression ratios of MAP1B mRNA were calculated by the formula: $2^{\Delta Ct}$, where ΔCt stands for the Ct (PCR cycle number when the signal reached the threshold) difference between groups. The filled bar represents average percentage expression of control (open bar, LC1-ATS untreated group). *D*, the effect of LC1-ATS on 5-HT$_{3A}$ receptor activation by LC1-ATS. Trace records of the current activated by 30 μM 5-HT are normalized. Bar graph represents average activation kinetics for 5-HT. *E*, modulation of 5-HT$_{3A}$ receptor desensitization by LC1-ATS. Trace records show decay of current in the presence of 30 μM 5-HT without (Ctr) and with pretreatment with LC1-ATS and inverted control. Bar graph represents average desensitization kinetics for 5-HT. Asterisk indicates a significant difference from control (unpaired *t* test, $P < 0.01$).

The current decay was normalized using a weighted summation of the fast and slow components as described in Methods. Nocodazole treatment abolished the fast component of the desensitization time constant. As illustrated in Fig. 6*B*, a single component of receptor desensitization was 6.2 ± 0.5 s in cells after nocodazole, which was nearly 6-fold slower than that of control (0.9 ± 0.1 s). In N1E115 cells treated with nocodazole, the activation (10.4 ± 0.4 ms *versus* 10.9 ± 0.4 ms) and deactivation time remained unchanged (3.6 ± 0.4 s *versus* 3.8 ± 0.2 s). To explore the mechanism underlying the nocodazole-induced effect, we conducted noise analysis to examine the unitary conductance of homomeric 5-HT_{3A} receptor–channels after nocodazole treatment. Consistent with previous results obtained under similar conditions (Brown *et al.* 1998), the unitary conductance of 5-HT_{3A} receptor–channels was 1.26 ± 0.119 pS (Fig. 6*C*). In cells treated with nocodazole, the unitary conductance was 1.09 ± 0.135 pS, which was not significantly different from the control value (Fig. 6*D*; $P > 0.05$, *t* test, $n = 7$).

Both LC1 and GABARAP increase microtubule stability against nocodazole

One likely mechanism by which nocodazole alters 5-HT_{3A} receptor gating is to destabilize microtubules. To test this hypothesis, we examined the extent of microtubule stability by measuring the levels of acetylated α-tubulin since stable microtubule polymers are enriched with acetylated α-tubulin in living cells, whereas unstable microtubule polymers and soluble tubulin dimers are devoid of acetylated α-tubulin. Consistent with previous studies (Takemura *et al.* 1992; Rochlin *et al.* 1996), pretreatment with nocodoazole (Noc) significantly reduced the level of acetylated tubulin (Fig. 7*A* and *B*; $P < 0.001$, $n = 4$). On the other hand, expression of LC1 and GABARAP significantly increased the levels of acetylated α-tubulin. Moreover, both LC1 and GABARAP completely reversed nocodazole-induced reduction of acetylated α-tubulin.

LC1 but not GABARAP rescues 5-HT_{3A} receptor desensitization after nocodazole treatment

The above observations have suggested that both LC1 and GABARAP can increase the resistance of microtubules to nocodazole in HEK 293 cells. We next asked if LC1 and GABARAP can reverse nocodazole-induced slow desensitization. Consistent with the above observation, 5-HT_{3A} receptor desensitization kinetics accelerated substantially when coexpressed with LC1 in HEK 293 cells (Fig. 8*A*). However, pretreatment of these cells

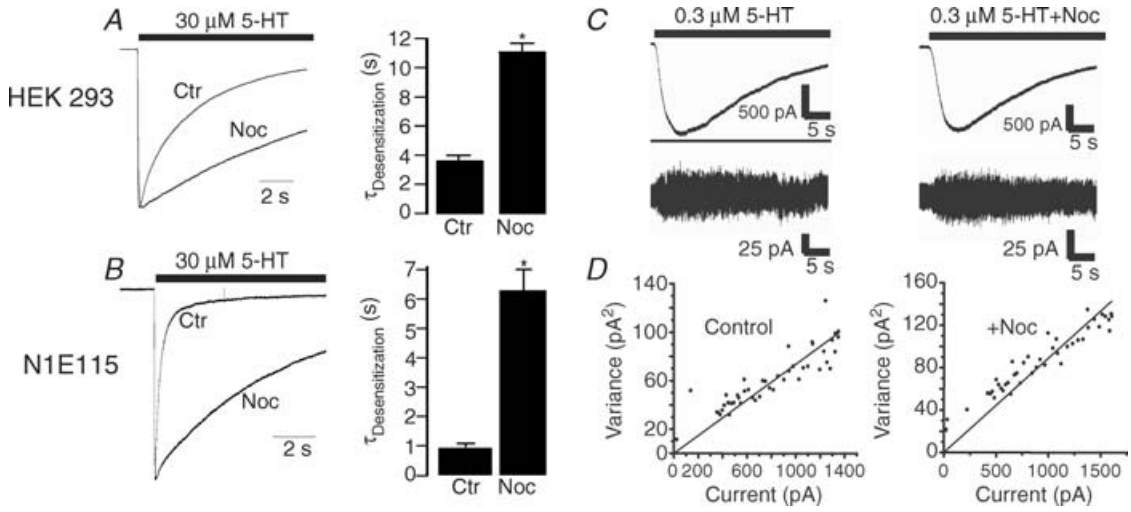

Figure 6. Pretreatment with nocodazole slows desensitization kinetics of the cloned and native 5-HT_3 receptors

A, normalized traces show receptor desensitization to a 10 s application of 30 μM 5-HT without and with pretreatment with 10 μM nocodazole (Noc) for 4 h in HEK 293 cells expressing 5-HT_{3A} receptors. Bar graph represents average desensitization kinetics for 5-HT ($n = 5$). Asterisk indicates a significant difference from control group (ANOVA, $P < 0.01$). *B*, traces show receptor desensitization to a 10 s application of 30 μM 5-HT without and with pretreatment with 10 μM Noc for 4 h in N1E115 cells. Bar graph represents average desensitization kinetics for 5-HT ($n = 5$). Asterisk indicates a significant difference from control group (ANOVA, $P < 0.01$). *C*, noise analysis of the effects of Noc treatment on single-channel conductance in HEK 293 cells expressing the 5-HT_{3A} subunits. Traces are records of current activated by 0.3 μM 5-HT in cells expressing the 5-HT_{3A} subunits without and with nocodazole treatment. *D*, variance *versus* current amplitude plots for the current records from individual cells. Single-channel conductance values from these cells were 1.12 pS for the control cell and 1.16 pS for the nocodazole-treated cell.

with nocodazole (Noc) did not alter the receptor desensitization kinetics (Fig. 8*A*), suggesting that LC1 can fully reverse the nocodazole-induced effect. In contrast, such a rescue was not observed in cells expressing GABARAP. In this case, GABARAP neither significantly affected receptor desensitization kinetics nor reversed the nocodazole-induced effect on receptor desensitization kinetics (Fig. 8*B*).

Discussion

In the study presented here, we have identified an interaction between the intracellular domain of the 5-HT$_{3A}$ receptor and LC1 in the yeast expression system. We have also demonstrated that LC1 was colocalized with the 5-HT$_{3A}$ subunits in hippocampal neurons, especially in growth cones, cohesion spots and dendrities. Similarly, LC1 and 5-HT$_{3A}$ subunits were colocalized in the microstructures such as lamellipodia and filapodia of HEK 293 cells. The functional consequence of the 5-HT$_{3A}$ receptor–LC1 interaction contributes to 5-HT$_{3A}$ receptor desensitization mechanisms. Particularly, LC1 accelerated 5-HT$_{3A}$ receptor desensitization kinetics and prevented nocodazole-induced kinetic change.

The interaction with LC1 appears to be selective for 5-HT$_{3A}$ subunits since no such interaction occurred in the 5-HT$_{3B}$ and GABA$_C$ subunits even though the GABA$_C$ subunit has been described to interact with the heavy chain of MAP1B (Hanley *et al.* 1999; Billups *et al.* 2000). Consistent with this idea, we observed that although both LC1 and GABARAP increased the resistance of microtubules against nocodazole treatment, only LC1 accelerated 5-HT$_{3A}$ receptor desensitization kinetics and prevented nocodazole-induced kinetic change. Moreover, disruption of the LC1–5-HT$_3$ receptor interaction by LC1-ATS significantly slowed desensitization kinetics. One possible mechanism is that LC directly targets 5-HT$_3$ receptors to microtubules. However, because of lacking direct evidence from coimmunoprecipitation experiments in brain tissues, we cannot exclude the possibility that LC1 may also link microtubules to other cytoskeleton proteins, thereby modulating 5-HT$_{3A}$ receptor function. For instance, LC1 was found to colocalize with 5-HT$_{3A}$ receptors in F-actin-rich domains of neurons and HEK 293 cell membrane (Emerit *et al.* 2002).

We have been unable to prove if LC1 can be co-precipitated with 5-HT$_3$ receptor proteins in brain tissues. There are a number of reasons to explain this failure. First, the antibodies that we used were unable to produce a strong signal for 5-HT$_3$ receptor proteins in brain tissues even though these antibodies have been used

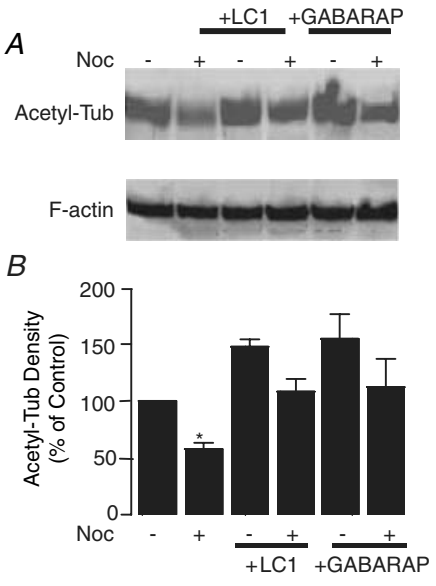

Figure 7. Increase of microtubule stability against nocodazole treatment by LC1 and GABA$_A$ receptor-associated protein (GABARAP)
A, Western blot of acetylated α-tubulin in HEK 293 cells expressing LC1 without and with nocodazole treatment (Noc). *B*, normalized average density of acetylated α-tubulin proteins. Each data point represents at least 4 samples. Asterisk indicates a significant difference from control (unpaired *t* test, $P < 0.01$).

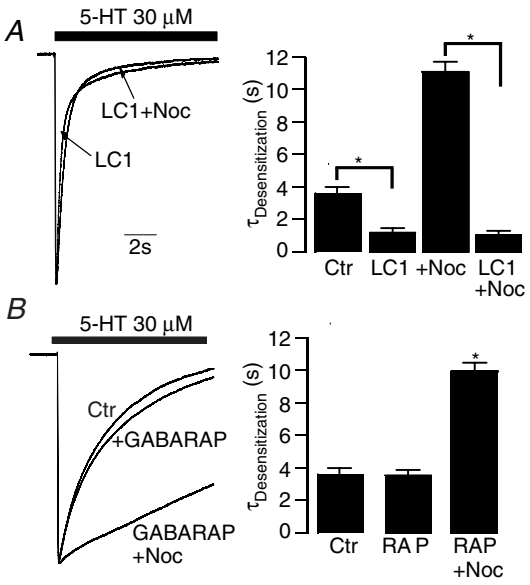

Figure 8. Rescue of 5-HT$_{3A}$ receptor desensitization kinetics by LC1 after nocodazole treatment
A, trace records of the normalized peak current show decay of current in the presence of 30 μM 5-HT in cells coexpressing 5-HT$_{3A}$ receptors and LC1 without and with nocodazole treatment (Noc). Bar graph represents average desensitization kinetics for 5-HT. ($n = 5$). Asterisk indicates a significant difference between two groups (ANOVA, $P < 0.001$). *B*, trace records show decay of current in the presence of 30 μM 5-HT in cells coexpressing 5-HT$_{3A}$ receptors and GABARAP (RAP) without and with nocodazole treatment. Bar graph represents average desensitization kinetics for 5-HT ($n = 5$). Asterisk indicates a significant difference from control (Ctr) and RAP groups (ANOVA, $P < 0.01$).

successfully in Western blots of 5-HT_3 receptor proteins expressed in *Xenopus* oocytes and HEK 293 cells (Sun *et al.* 2003). This observation suggests that the expression level of 5-HT_{3A} receptor proteins in the whole brain may be relatively low. Consistent with this idea, 5-HT-activated currents are either small or rarely seen in most of the central neurons isolated from rodent brains (Sung *et al.* 2000). Second, native 5-HT_{3A} receptors are likely to exist in degraded forms, especially in nervous tissues. For instance, Western blots of native 5-HT_{3A} receptors in brain tissues have always revealed a dominant band at 35 kDa (Miquel *et al.* 1990; Fletcher & Barnes, 1997; Spier *et al.* 1999). The protein degradation could impair the interaction between the 5-HT_{3A} receptor and LC1. Third, the interaction between the 5-HT_3 receptor and LC1 could be transient and dynamic, which could limit the ability of coimmunoprecipitation to detect LC1–receptor interaction. Finally, we cannot totally rule out the possibility that a third protein is required for the 5-HT_{3A} receptor to interact with the LC1 in mammalian brain tissues.

The key finding of this study is that LC1 plays a role in the regulation of 5-HT_3 receptor desensitization. The precise mechanism of such regulation is unclear. It is proposed that the agonist affinity of a given receptor in the desensitized state is higher than that in the non-desensitized closed state. Consistent with this idea, both GABARAP and MAP1B have been found to change the sensitivity of $GABA_A$ and $GABA_C$ receptors to GABA (Billups *et al.* 2000; Chen *et al.* 2000), suggesting that the functional modulation of the channels results from a decreased sensitivity of the receptors to agonist. However, it is unlikely to be the same case in 5-HT_{3A} receptors as LC1 did not significantly affect receptor binding affinity. One likely mechanism is that LC1 regulates 5-HT_{3A} receptor desensitization kinetics by reducing cell surface receptor density. This is consistent with many recent studies of channel–cytoskeleton interaction in which decrease or increase in the surface fraction of receptors may alter receptor gating kinetics (Billups *et al.* 2000; Chen *et al.* 2000; Leil *et al.* 2004; Boileau *et al.* 2005; Chen *et al.* 2005). We noted that there are a few differences in the modulation of $GABA_C$ and 5-HT_3 receptors by MAP1B. For instance, the heavy chain of MAP1B has been shown to alter the sensitivity of $GABA_C$ receptors to agonist (Billups *et al.* 2000), whereas LC1 did not significantly affect the apparent agonist affinity for 5-HT_3 receptors.

5-HT_{3A} receptors are located postsynaptically and also presynaptically, where they modulate the release of other neurotransmitters (Miquel *et al.* 2002). So far, the routing mechanism of these receptors towards the nerve terminals is unknown. 5-HT_{3A} receptor clusters have been described to follow the tubulin and F-actin networks for receptor routing and precise tuning at the neuron membrane surface (Emerit *et al.* 2002; Grailhe *et al.* 2004; Ilegems *et al.* 2004). MAP1B consists of a heavy chain and a light chain (LC1) with a ratio of 1 : 7 in the brain (Noble *et al.* 1989; Hammarback *et al.* 1991). Although MAP1B is predominantly expressed in the central and peripheral nervous systems at an early developmental stage, MAP1B is also detected in postsynaptic dendrites at the adult stage (Noble *et al.* 1989; Hammarback *et al.* 1991; Bouquet *et al.* 2004; Szebenyi *et al.* 2005). In addition, MAP1B is highly expressed in neurons isolated from dorsal root ganglia at the adult stage (Meixner *et al.* 2000; Bouquet *et al.* 2004). It should be interesting for future studies to determine whether or not LC1 could contribute to the routing mechanisms of 5-HT_3 receptors in the central nervous system.

In conclusion, our observations have suggested that LC1 can modulate 5-HT_{3A} receptor desensitization kinetics through a possible direct interaction. Such channel–cytoskeleton interaction may be critical for transporting 5-HT_{3A} receptors into presynaptic sites. Modulation of 5-HT_3 receptor desensitization by LC1 could contribute to reshaping the efficacy of 5-HT_{3A} receptor-mediated neurotransmission in pre- and postsynaptic areas. Our results presented here should open a new avenue for future studies to address the physiological and pathological roles of the cytoskeleton proteins in regulating 5-HT_{3A} receptor function.

References

Betz H (1990). Ligand-gated ion channels in the brain: the amino acid receptor superfamily. *Neuron* **5**, 383–392.

Billups D, Hanley JG, Orme M, Attwell D & Moss SJ (2000). $GABA_C$ receptor sensitivity is modulated by interaction with MAP1B. *J Neurosci* **20**, 8643–8650.

Bohler S, Gay S, Bertrand S, Corringer PJ, Edelstein SJ, Changeux JP & Bertrand D (2001). Desensitization of neuronal nicotinic acetylcholine receptors conferred by N-terminal segments of the β_2 subunit. *Biochemistry* **40**, 2066–2074.

Boileau AJ, Pearce RA & Czajkowski C (2005). Tandem subunits effectively constrain $GABA_A$ receptor stoichiometry and recapitulate receptor kinetics but are insensitive to $GABA_A$ receptor-associated protein. *J Neurosci* **25**, 11219–11230.

Bouquet C, Soares S, von Boxberg Y, Ravaille-Veron M, Propst F & Nothias F (2004). Microtubule-associated protein 1B controls directionality of growth cone migration and axonal branching in regeneration of adult dorsal root ganglia neurons. *J Neurosci* **24**, 7204–7213.

Brown AM, Hope AG, Lambert JJ & Peters JA (1998). Ion permeation and conduction in a human recombinant 5-HT_3 receptor subunit (h5-HT_{3A}). *J Physiol* **507**, 653–665.

Chen ZW, Chang CS, Leil TA, Olcese R & Olsen RW (2005). $GABA_A$ receptor-associated protein regulates $GABA_A$ receptor cell-surface number in *Xenopus laevis* oocytes. *Mol Pharmacol* **68**, 152–159.

Chen ZW & Olsen RW(2007). $GABA_A$ receptor associated proteins: a key factor regulating $GABA_A$ receptor function. *J Neurochem* **100**, 279–294.

Chen L, Wang H, Vicini S & Olsen RW (2000). The γ-aminobutyric acid type A ($GABA_A$) receptor-associated protein (GABARAP) promotes $GABA_A$ receptor clustering and modulates the channel kinetics. *Proc Natl Acad Sci U S A* **97**, 11557–11562.

Corringer PJ, Bertrand S, Bohler S, Edelstein SJ, Changeux JP & Bertrand D (1998). Critical elements determining diversity in agonist binding and desensitization of neuronal nicotinic acetylcholine receptors. *J Neurosci* **18**, 648–657.

Del Rio JA, Gonzalez-Billault C, Urena JM, Jimenez EM, Barallobre MJ, Pascual M, Pujadas L, Simo S, La Torre A, Wandosell F, Avila J & Soriano E (2004). MAP1B is required for Netrin 1 signaling in neuronal migration and axonal guidance. *Curr Biol* **14**, 840–850.

Emerit MB, Doucet E, Darmon M & Hamon M (2002). Native and cloned 5-HT_{3A} (S) receptors are anchored to F-actin in clonal cells and neurons. *Mol Cell Neurosci* **20**, 110–124.

Everitt AB, Luu T, Cromer B, Tierney ML, Birnir B, Olsen RW & Gage PW (2004). Conductance of recombinant $GABA_A$ channels is increased in cells co-expressing $GABA_A$ receptor-associated protein. *J Biol Chem* **279**, 21701–21706.

Fletcher S & Barnes NM (1997). Purification of 5-hydroxytryptamine$_3$ receptors from porcine brain. *Br J Pharmacol* **122**, 655–662.

Grailhe R, de Carvalho LP, Paas Y, Le Poupon C, Soudant M, Bregestovski P, Changeux JP & Corringer PJ (2004). Distinct subcellular targeting of fluorescent nicotinic $\alpha 3\beta 4$ and serotoninergic 5-HT_{3A} receptors in hippocampal neurons. *Eur J Neurosci* **19**, 855–862.

Gunthorpe MJ, Peters JA, Gill CH, Lambert JJ & Lummis SC (2000). The 4′lysine in the putative channel lining domain affects desensitization but not the single-channel conductance of recombinant homomeric 5-HT_{3A} receptors. *J Physiol* **522**, 187–198.

Hammarback JA, Obar RA, Hughes SM & Vallee RB (1991). MAP1B is encoded as a polyprotein that is processed to form a complex N-terminal microtubule-binding domain. *Neuron* **7**, 129–139.

Hanley JG, Koulen P, Bedford F, Gordon-Weeks PR & Moss SJ (1999). The protein MAP-1B links $GABA_C$ receptors to the cytoskeleton at retinal synapses. *Nature* **397**, 66–69.

Hu XQ, Sun H, Peoples RW, Hong R & Zhang L (2006). An interaction involving an arginine residue in the cytoplasmic domain of the 5-HT_{3A} receptor contributes to receptor desensitization mechanism. *J Biol Chem* **281**, 21781–21788.

Hu XQ, Zhang L, Stewart RR & Weight FF (2003). Arginine 222 in the pre-transmembrane domain 1 of 5-HT_{3A} receptors links agonist binding to channel gating. *J Biol Chem* **278**, 46583–46589.

Ilegems E, Pick HM, Deluz C, Kellenberger S & Vogel H (2004). Noninvasive imaging of 5-HT_3 receptor trafficking in live cells: from biosynthesis to endocytosis. *J Biol Chem* **279**, 53346–53352.

Jones MV & Westbrook GL (1995). Desensitized states prolong $GABA_A$ channel responses to brief agonist pulses. *Neuron* **15**, 181–191.

Jones MV & Westbrook GL (1996). The impact of receptor desensitization on fast synaptic transmission. *Trends Neurosci* **19**, 96–101.

Kawakami S, Muramoto K, Ichikawa M & Kuroda Y (2003). Localization of microtubule-associated protein (MAP) 1B in the postsynaptic densities of the rat cerebral cortex. *Cell Mol Neurobiol* **23**, 887–894.

Kirsch J, Wolters I, Triller A & Betz H (1993). Gephyrin antisense oligonucleotides prevent glycine receptor clustering in spinal neurons. *Nature* **366**, 745–748.

Leil TA, Chen ZW, Chang CS & Olsen RW (2004). $GABA_A$ receptor-associated protein traffics $GABA_A$ receptors to the plasma membrane in neurons. *J Neurosci* **24**, 11429–11438.

Lopez I & McKay DB (1997). Effects of antimitotic agents on secretion and detergent extractibility of adrenal nicotinic acetylcholine receptors. *Cell Mol Neurobiol* **17**, 447–454.

Luu T, Gage PW & Tierney ML (2006). GABA increases both the conductance and mean open time of recombinant $GABA_A$ channels co-expressed with GABARAP. *J Biol Chem* **281**, 35699–35708.

Maricq AV, Peterson AS, Brake AJ, Myers RM & Julius D (1991). Primary structure and functional expression of the $5HT_3$ receptor, a serotonin-gated ion channel. *Science* **254**, 432–437.

Meixner A, Haverkamp S, Wassle H, Fuhrer S, Thalhammer J, Kropf N, Bittner RE, Lassmann H, Wiche G & Propst F (2000). MAP1B is required for axon guidance and is involved in the development of the central and peripheral nervous system. *J Cell Biol* **151**, 1169–1178.

Miquel MC, Emerit MB, Bolanos FJ, Schechter LE, Gozlan H & Hamon M (1990). Physicochemical properties of serotonin 5-HT_3 binding sites solubilized from membranes of NG 108-15 neuroblastoma-glioma cells. *J Neurochem* **55**, 1526–1536.

Miquel MC, Emerit MB, Nosjean A, Simon A, Rumajogee P, Brisorgueil MJ, Doucet E, Hamon M & Verge D (2002). Differential subcellular localization of the 5-HT_3-As receptor subunit in the rat central nervous system. *Eur J Neurosci* **15**, 449–457.

Moss SJ & Smart TG (2001). Constructing inhibitory synapses. *Nat Rev Neurosci* **2**, 240–250.

Noble M, Lewis SA & Cowan NJ (1989). The microtubule binding domain of microtubule-associated protein MAP1B contains a repeated sequence motif unrelated to that of MAP2 and tau. *J Cell Biol* **109**, 3367–3376.

Ortells MO & Lunt GG (1995). Evolutionary history of the ligand-gated ion-channel superfamily of receptors. *Trends Neurosci* **18**, 121–127.

Overstreet LS, Jones MV & Westbrook GL (2000). Slow desensitization regulates the availability of synaptic $GABA_A$ receptors. *J Neurosci* **20**, 7914–7921.

Petrini EM, Zacchi P, Barberis A, Mozrzymas JW & Cherubini E (2003). Declusterization of $GABA_A$ receptors affects the kinetic properties of GABAergic currents in cultured hippocampal neurons. *J Biol Chem* **278**, 16271–16279.

Rochlin MW, Wickline KM & Bridgman PC (1996). Microtubule stability decreases axon elongation but not axoplasm production. *J Neurosci* **16**, 3236–3246.

Sheng M & Pak DT (2000). Ligand-gated ion channel interactions with cytoskeletal and signaling proteins. *Annu Rev Physiol* **62**, 755–778.

Spier AD, Wotherspoon G, Nayak SV, Nichols RA, Priestley JV & Lummis SC (1999). Antibodies against the extracellular domain of the 5-HT_3 receptor label both native and recombinant receptors. *Brain Res Mol Brain Res* **67**, 221–230.

Sun H, Hu XQ, Moradel EM, Weight FF & Zhang L (2003). Modulation of 5-HT_3 receptor-mediated response and trafficking by activation of protein kinase C. *J Biol Chem* **278**, 34150–34157.

Sun Y, Olson R, Horning M, Armstrong N, Mayer M & Gouaux E (2002). Mechanism of glutamate receptor desensitization. *Nature* **417**, 245–253.

Sung KW, Engel SR, Allan AM & Lovinger DM (2000). 5-HT_3 receptor function and potentiation by alcohols in frontal cortex neurons from transgenic mice overexpressing the receptor. *Neuropharmacology* **39**, 2346–2351.

Szebenyi G, Bollati F, Bisbal M, Sheridan S, Faas L, Wray R, Haferkamp S, Nguyen S, Caceres A & Brady ST (2005). Activity-driven dendritic remodeling requires microtubule-associated protein 1A. *Curr Biol* **15**, 1820–1826.

Takemura R, Okabe S, Umeyama T, Kanai Y, Cowan NJ & Hirokawa N (1992). Increased microtubule stability and alpha tubulin acetylation in cells transfected with microtubule-associated proteins MAP1B, MAP2 or tau. *J Cell Sci* **103**, 953–964.

Van Hooft JA & Vijverberg HP (1995). Phosphorylation controls conductance of 5-HT_3 receptor ligand-gated ion channels. *Receptors Channels* **3**, 7–12.

van Hooft JA & Vijverberg HP (2000). 5-HT_3 receptors and neurotransmitter release in the CNS: a nerve ending story? *Trends Neurosci* **23**, 605–610.

van Rossum D, Kuhse J & Betz H (1999). Dynamic interaction between soluble tubulin and C-terminal domains of *N*-methyl-D-aspartate receptor subunits. *J Neurochem* **72**, 962–973.

Van Zundert B, Alvarez FJ, Tapia JC, Yeh HH, Diaz E & Aguayo LG (2004). Developmental-dependent action of microtubule depolymerization on the function and structure of synaptic glycine receptor clusters in spinal neurons. *J Neurophysiol* **91**, 1036–1049.

Wang H, Bedford FK, Brandon NJ, Moss SJ & Olsen RW (1999). $GABA_A$-receptor-associated protein links $GABA_A$ receptors and the cytoskeleton. *Nature* **397**, 69–72.

Washbourne P, Liu XB, Jones EG & McAllister AK (2004). Cycling of NMDA receptors during trafficking in neurons before synapse formation. *J Neurosci* **24**, 8253–8264.

Yakel JL & Jackson MB (1988). 5-HT_3 receptors mediate rapid responses in cultured hippocampus and a clonal cell line. *Neuron* **1**, 615–621.

Yuen EY, Jiang Q, Feng J & Yan Z (2005). Microtubule regulation of *N*-methyl-D-aspartate receptor channels in neurons. *J Biol Chem* **280**, 29420–29427.

Zhang L & Lummis SC (2006). *5-HT_3 Receptors*, chapter 6, 135–154, Taylor & Francis Group, LLC., New York, NY 10016.

Acknowledgements

We thank Drs D. Julius, J. A. Hammarback and J. P. Changeux for providing us with the cDNAs of mouse 5-HT_{3A} subunit, rat LC1 and mouse YFP-5-HT_{3A} subunit, respectively. We thank Dr S. C. Lummis for providing us with a specific antibody against the 5-HT_{3A} receptor. We thank Dr D. M. Lovinger for comments on this manuscript. This study was supported by the NIAAA Division of Intramural Clinical and Basic Research.